

Fermi-liquid behavior and weakly anisotropic superconductivity in the electron-doped cuprate $\text{Sr}_{1-x}\text{La}_x\text{CuO}_2$

Kohki H. Satoh,^{1,*} Soshi Takeshita,² Akihiro Koda,^{1,2} Ryosuke Kadono,^{1,2} Kenji Ishida,³ Sunsen Pyon,⁴ Takao Sasagawa,^{4,†} and Hidenori Takagi⁴

¹Department of Materials Structure Science, The Graduate University for Advanced Studies, Tsukuba, Ibaraki 305-0801, Japan

²Institute of Materials Structure Science, High Energy Accelerator Research Organization, Tsukuba, Ibaraki 305-0801, Japan

³Department of Physics, Graduate School of Science, Kyoto University, Kyoto 606-8502, Japan

⁴Department of Advanced Materials Science, University of Tokyo, Kashiwa, Chiba 277-8561, Japan

(Received 14 September 2007; revised manuscript received 26 March 2008; published 9 June 2008)

The microscopic details of flux-line lattice state studied by muon spin rotation are reported in an electron-doped high- T_c cuprate superconductor, $\text{Sr}_{1-x}\text{La}_x\text{CuO}_2$ (SLCO) ($x=0.10-0.15$). A clear sign of phase separation between magnetic and nonmagnetic phases is observed, where the effective magnetic penetration depth [$\lambda \equiv \lambda(T, H)$] is determined selectively for the latter phase. The extremely small value of $\lambda(0, 0)$ and corresponding large superfluid density ($n_s \propto \lambda^{-2}$) is consistent with the presence of a large Fermi surface with carrier density of $1+x$, which suggests the breakdown of the “doped Mott insulator” even at the “optimal doping” in SLCO. Moreover, a relatively weak anisotropy in the superconducting order parameter is suggested by the field dependence of $\lambda(0, H)$. These observations strongly suggest that the superconductivity in SLCO is of a different class from hole-doped cuprates.

DOI: [10.1103/PhysRevB.77.224503](https://doi.org/10.1103/PhysRevB.77.224503)

PACS number(s): 74.25.Qt, 74.72.-h, 76.75.+i

The question whether or not the mechanism of superconductivity in electron-doped (n -type) cuprates is common to that in hole-doped (p -type) cuprates is one of the most interesting issues in the field of cuprate superconductors, which is yet to be answered. This “electron-hole symmetry” has been addressed by many experiments and theories since the discovery of n -type cuprate superconductors.¹ In the theoretical models assuming strong electronic correlation where the infinitely large on-site Coulomb interaction ($U \rightarrow \infty$) leads to the Mott insulating phase for the half filled band, the correlation among the doped carriers is projected into the t - J model in which the mechanism of superconductivity does not depend on the sign of charge carriers.^{2,3} This is in marked contrast to the models starting from Fermi-liquid (=normal metal) state, where such symmetry is irrelevant to their basic framework.⁴ Experimentally, recent advent in crystal-growth techniques and that in experimental methods for evaluating their electronic properties triggered detailed measurements on n -type cuprates, reporting interesting results suggesting certain differences from p -type ones, such as the observation of a commensurate spin fluctuations in neutron-scattering study or the nonmonotonic d -wave superconducting order parameter in angle-resolved photoelectron spectroscopy (ARPES) measurement.^{5,6}

The effective magnetic penetration depth (λ) is one of the most important physical quantities directly related to the superfluid density (n_s),

$$\frac{1}{\lambda^2} = \frac{n_s e^2}{m^* c}, \quad (1)$$

which is reflected in the microscopic field profile of the flux-line lattice (FLL) state in type II superconductors. Considering that the response of n_s against various perturbations strongly depends on the characters of the Cooper pairing, the comparison of n_s between two types of carriers might serve

as a testing ground for the electron-hole symmetry. However, the study of FLL state in n -type cuprates such as T' -phase RE_2CuO_4 compounds (RE=Nd, Pr, Sm, etc.) is far behind that in p -type cuprates because of strong random local fields from rare-earth ions which mask information of CuO_2 planes regarding both superconductivity and magnetism against magnetic probes such as muon. In this regard, infinite-layer structured $\text{Sr}_{1-x}\text{La}_x\text{CuO}_2$ (SLCO) is a suitable compound for detailed muon spin relaxation and rotation (μSR) study of electron-doped systems, as it is free from magnetic rare-earth ions.

A recent μSR study on SLCO with $x=0.10$ ($T_c \approx 40$ K) reported a relatively large $n_s \propto \lambda_{ab}^{-2}$ [$\lambda_{ab}(T \rightarrow 0) \sim 116$ nm] as compared to p -type cuprates,⁷ strongly suggesting that n -type cuprates belong to a different class in view of the n_s versus T_c relation.⁸ On the other hand, another μSR study showed the appearance of a spin-glass-like magnetism over a wide temperature range including superconducting phase,⁹ which might have also affected the result of Ref. 7. In this paper, we demonstrate by μSR measurements under both zero field (ZF) and high transverse field (HTF) that SLCO exhibits a phase separation into magnetic and nonmagnetic phases, where the superconductivity occurs predominantly in the latter. Our measurement made it feasible to evaluate λ reliably as it was selectively determined for the nonmagnetic phase of SLCO.

Meanwhile, the pairing symmetry of order parameter, which is one of the most important issues in discussing the electron-hole symmetry, still remains controversial in n -type cuprates. A number of groups reported s -wave symmetry in SLCO,^{10,11} which is in marked contrast to the $d_{x^2-y^2}$ symmetry well established in p -type cuprates. The pairing symmetry can be examined by measuring the temperature and/or field variation of $\lambda(T, H)$ as an *effective* value observed by μSR : it reflects the change in $n_s \equiv n_s(T, H)$ due to quasiparticle excitation and/or nonlocal effect associated with anisotropic or-

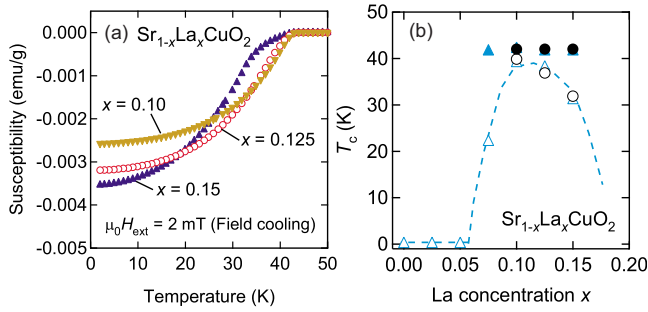


FIG. 1. (Color online) (a) Magnetic susceptibility of SLCO with $x=0.10, 0.125,$ and 0.15 under 20 G. (b) La concentration dependence of T_c . The closed symbols show $T_{c\text{onset}}$ and the open symbols show $T_{c\text{bulk}}$, respectively. An earlier result (Ref. 15) (triangles) is also quoted for comparison. The dashed line is guide for the eyes.

der parameter.^{12,13} Here, we show evidence that the order parameter in SLCO is not described by simple isotropic s -wave pairing nor that of pure $d_{x^2-y^2}$.

Powder samples of SLCO ($x=0.10, 0.125,$ and 0.15) were prepared by high-pressure synthesis under 6 GPa at 1000 °C. They were confirmed to be of single phase by powder x-ray diffraction, where a small amount of $\text{LaCuO}_{2.5}$ phase (LCO2.5, less than a few percent) was identified. The length of a and c axes showed almost linear change with x , indicating successful substitution of Sr with La for carrier doping.¹⁴ As displayed in Fig. 1(a), the susceptibility (χ_0) measured by superconducting quantum interference device magnetometer implies that the onset of superconductivity is nearly 42 K and least dependent on x , whereas the bulk T_c determined by the maximum of $d\chi_0/dT$ varies with x [see Fig. 1(b)], which reproduces earlier results.^{15,16} The x dependence of bulk T_c suggests that the sample is close to the optimal doping for $x=0.1$.

The μSR experiment was performed on the M15 beamline at TRIUMF (Vancouver, Canada), where measurements under ZF and longitudinal field (LF) were made to investigate magnetic ground state of SLCO. Subsequently, those under a HTF (up to 6 T) were made to study the FLL state in detail. In ZF and LF measurements, a pair of scintillation counters (in backward and forward geometry relative to the initial muon polarization that was parallel to the beam direc-

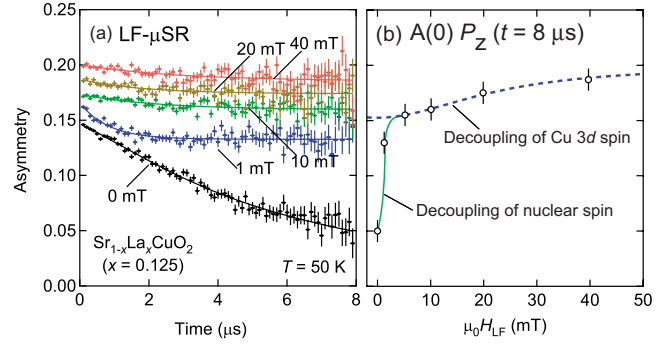


FIG. 3. (Color online) (a) LF- μSR spectra in the sample with $x=0.125$. (b) Two kinds of decoupling behavior at 50 K. The dashed line is fitting curb by Eq. (2)

tion) were employed for the detection of positron emitted preferentially to the muon polarization upon its decay. In HTF measurements, sample was at the center of four position counters placed around the beam axis, and initial muon spin polarization was perpendicular to the muon beam direction so that the magnetic field can be applied along the beam direction without interfering with beam trajectory. A veto countersystem was employed to eliminate background signals from the muons that missed the sample, which was crucial for samples available only in small quantities such as those obtained by high-pressure synthesis. For the measurements under a transverse field, the sample was field-cooled to the target temperature to minimize the effect of flux pinning.

Figure 2(a) shows ZF- μSR spectra for the sample with $x=0.125$, where no spontaneous muon precession is observed as sample is cooled down to 2 K. Instead, fast muon spin depolarization can be identified between $0 < t < 0.2 \mu\text{s}$, which develops with decreasing temperature. LF- μSR spectra in Fig. 3(a) show that the depolarization is quenched in two steps as a function of field strength, at first near a few millitesla due to nuclear magnetic moments and second around 10^1 mT. The asymptotic behavior of $P_z(t)$ under random local fields H (with an isotropic mean square, $\langle H_x^2 \rangle = \langle H_y^2 \rangle = \langle H_z^2 \rangle = \frac{1}{3} \langle H^2 \rangle$) as a function of external magnetic field H_{LF} is approximately given by the following equation:

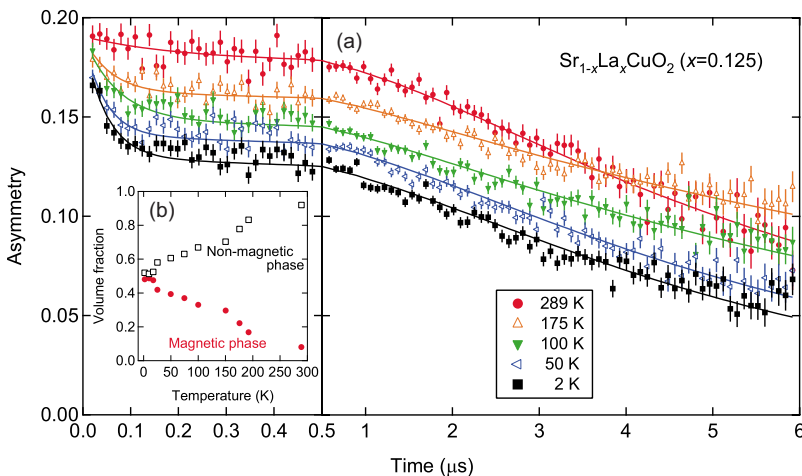


FIG. 2. (Color online) (a) ZF- μSR spectra in the sample with $x=0.125$. Inset (b) is temperature dependence of the volume fraction of magnetic and nonmagnetic phases.

$$P_z(t \rightarrow \infty) \approx \frac{H_{\text{LF}}^2 + \langle H_z^2 \rangle}{H_{\text{LF}}^2 + \langle H^2 \rangle} = \frac{H_{\text{LF}}^2 + \frac{1}{3} \langle H^2 \rangle}{H_{\text{LF}}^2 + \langle H^2 \rangle}, \quad (2)$$

and we estimated the magnitude of $\sqrt{\langle H^2 \rangle} \equiv \bar{H}_{\text{int}}$ from the behavior of $P_z(t \rightarrow \infty)$ as 39(3) mT [the best fit with Eq. (2) is shown in Fig. 3(b)]. This is consistent with the fast initial depolarization rate estimated by $\gamma_\mu \bar{H}_{\text{int}} = 33(3)$ MHz (where $\gamma_\mu = 2\pi \times 135.53$ MHz/T is the muon gyromagnetic ratio). The origin of \bar{H}_{int} can be uniquely attributed to the localized moment of Cu atoms, where the effective moment size is $0.15(1)\mu_B$. The almost negligible depolarization for the asymptotic component implies that spin-fluctuation rate is much smaller than $\gamma_\mu \bar{H}_{\text{int}}$ at 50 K. Thus, ZF/LF- μ SR results strongly suggest that the sample that exhibits superconductivity has also static magnetic phase. The magnetic region enlarges to a halfway partition at low temperature [as seen in Fig. 2(b)]. We note that a common tendency was observed for $x=0.10$ and 0.15 .

In HTF- μ SR, each pair of counters (right-left, upward-downward) observes time-dependent muon spin polarization, $\hat{P}(t)$, projected to the x or y axis perpendicular to the beam direction (with a relative phase shift of $\pi/2$). Inhomogeneity of magnetic-field distribution $B(\mathbf{r})$ leads to depolarization due to the loss of phase coherence among muons probing different parts of $B(\mathbf{r})$. Using a complex notation, $\hat{P}(t)$ is directly provided using the spectral density distribution for the internal field, $n(B)$,

$$\hat{P}(t) = P_x(t) + iP_y(t) = \int_{-\infty}^{\infty} n(B) e^{i(\gamma_\mu B t - \phi)} dB, \quad (3)$$

where $n(B)$ is defined as a spatial average $\langle \delta \rangle_r$ of the delta function,

$$n(B) = \langle \delta[B - B(\mathbf{r})] \rangle_r, \quad (4)$$

and ϕ is the initial phase of muon spin rotation. Then, the real part of fast Fourier transform (FFT) of μ SR time spectra corresponds to $n(B)$, namely,

$$n(B) = \Re \int_{-\infty}^{\infty} \hat{P}(t) e^{-i(\gamma_\mu B t - \phi)} dt. \quad (5)$$

Figure 4 shows the real amplitudes obtained by the FFT of HTF- μ SR spectra, which contain information on $n(B)$. The narrow central peak (labeled A) is the signal from muons stopped in a nonmagnetic (and/or nonsuperconducting) phase where the frequency is equal to that of the external field ($\mu_0 H_{\text{ext}} = 6$ T) with a linewidth determined by random nuclear dipolar fields besides the effect of limited time window ($0 \leq t \leq 6 \mu\text{s}$). A broad satellite peak (labeled B) appears on the positive side of the central peak, when temperature is lowered below 300 K. This corresponds to the fast depolarization in time domain. The ZF/LF- μ SR spectra in Figs. 2 and 3 demonstrate that this satellite comes from a magnetic phase in which quasistatic random magnetism of Cu electron spins develops.

While the FFT spectra were useful to examine the overall feature of $n(B)$, the actual data analysis was carried out in

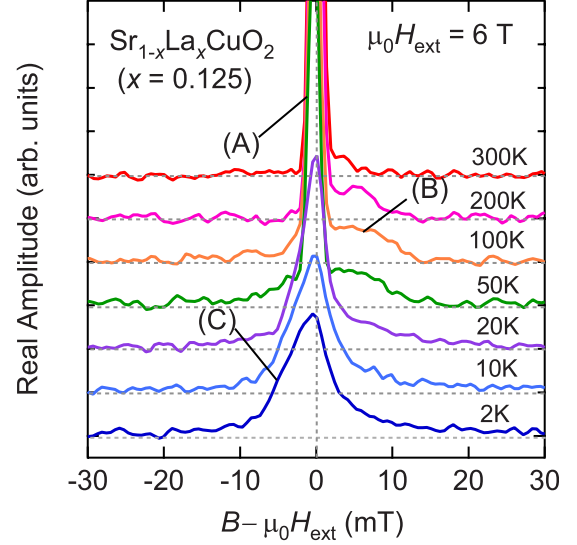


FIG. 4. (Color online) Fast Fourier transform of HTF- μ SR spectra under 6 T [after filtering the artifacts due to a finite time window for transform ($0 \leq t \leq 6 \mu\text{s}$)]. The peaks labeled A, B, and C correspond to nonmagnetic and/or nonsuperconducting, magnetic, and FLL phases, respectively.

time domain using the χ^2 -minimizing method. As inferred by Fig. 4, the μ SR spectra in the normal state can be reproduced by a sum of two Gaussian damping signals,

$$\begin{aligned} \hat{P}_n(t) &= \sum_{k=1}^2 f_k \int_{-\infty}^{\infty} n_k(B) e^{i(\gamma_\mu B t - \phi)} dB \\ &= \sum_{k=1}^2 f_k \exp(-\sigma_k^2 t^2 / 2) e^{i(\omega_k t - \phi)}, \end{aligned} \quad (6)$$

where f_k is the relative yield proportional to the fractional volume of each phase, σ_k is the linewidth, and $\omega_k = \gamma_\mu \bar{B}_k$, with \bar{B}_k being the mean value of local magnetic field following a Gaussian distribution,

$$n_k(B) = (\sqrt{2\pi}\sigma_k)^{-1} \exp[-\gamma_\mu^2 (B - \bar{B}_k)^2 / 2\sigma_k^2].$$

It is inferred from the χ^2 -minimizing fit of the time spectra by Eq. (6) that the volume fraction of magnetic phase increases toward low temperature monotonously in place of nonmagnetic phase and becomes nearly a half at 50 K. This is clearly not due to the LCO2.5 impurity phase, considering the small volume fraction of LCO2.5 and its known Néel temperature (~ 125 K).¹⁷ The magnetic volume fraction is independent of H_{ext} at 50 K where the sample is in the normal state. Thus, the appearance of the satellite peak demonstrates the occurrence of a phase separation into magnetic and nonmagnetic domains in the normal state of SLCO.

Taking the result in the normal state into consideration, we analyzed the μ SR spectra in the superconducting phase. In the FLL state of type II superconductors, one can reasonably assume that muon stops randomly over the length scale of vortex lattice and serves to provide a random sampling of inhomogeneity due to FLL formation. In the modified-

London (*m*-London) model, $B(\mathbf{r})$ is approximated as a sum of magnetic inductions from isolated vortices,

$$B_v(\mathbf{r}) = B_0 \sum_{\mathbf{K}} \frac{e^{-i\mathbf{K}\cdot\mathbf{r}}}{1 + K^2\lambda^2} F(K, \xi_v),$$

where \mathbf{K} are the vortex reciprocal-lattice vectors, B_0 ($\approx \mu_0 H_{\text{ext}}$) is the average internal field, $\lambda \equiv \lambda(T, H)$ is the effective London penetration depth depending on temperature and field, and $F(K, \xi_v) = \exp(-K^2 \xi_v^2 / 2)$ is a nonlocal correction term with ξ_v ($\approx \xi$) being the cutoff parameter for the magnetic-field distribution; the Gaussian cutoff generally provides satisfactory agreement with data. The density distribution $n(B)$ in this case is characterized by the Van Hove singularity originating from the saddle points of $B_v(\mathbf{r})$ with a negative shift primarily determined by λ and that corresponds to the peak (seen as a shoulder) labeled C in Fig. 4. Thus, the signal from the FLL state can be readily separated from other phases at large H_{ext} as they exhibit different frequency shifts with each other. The FFT spectra below T_c also indicate that the domain size of the superconducting phase is much greater than that determined by λ .

It is known that the *m*-London model is virtually identical to the Ginzburg-Landau (GL) model for large $\kappa = \lambda / \xi$ (ξ is the GL coherence length) and at low magnetic fields ($H_{\text{ext}} / H_{c2} < 0.25$, with H_{c2} being the upper critical field).^{18,19} Meanwhile, according to a reported value of the upper critical field for SLCO ($\mu_0 H_{c2} = 12$ T, in Ref. 20), the field range of the present measurements ($0 \leq \mu_0 H_{\text{ext}} \leq 6$ T) might exceed the above mentioned boundary, and thus the use of the GL model would be more appropriate. However, the *m*-London model has certain advantages over the GL model in practical application to the analysis: for example, we can avoid further complexity of analysis due to introduction of the field-dependent effective coherence length.¹² We also stress that the discrepancy in the analysis results has been studied in detail between these two models, and now it is well established that *m*-London model exhibits a systematic tendency of slight overestimation of λ at higher fields due to a known cause.^{12,19} The discussion on the present result will be made below considering this tendency.

Another uncertainty comes from the fact that the FLL symmetry in SLCO is not known at this stage, and it might even depend on the magnitude of external field as has been found in some other cuprates.^{21,22} However, since we do not observe any abrupt change in line shape nor the increase in χ^2 in the fits (irrespective of model) associated with the alteration of FLL symmetry with varying field,^{23,24} we can reasonably assume that the FLL symmetry remains the same throughout entire field range. Moreover, the observed line shape is perfectly in line with the hexagonal FLL, without showing any sign of squared FLL (e.g., a large spectral weight at the lower field side of the central peak in the absence of nonlocal effect²⁵ or an enhanced weight at the central peak associated with the strong nonlocal effect²⁴). Therefore, the FLL symmetry has been assumed to be hexagonal in the following analysis.

The μ SR spectra in the FLL state were analyzed by fit analysis using

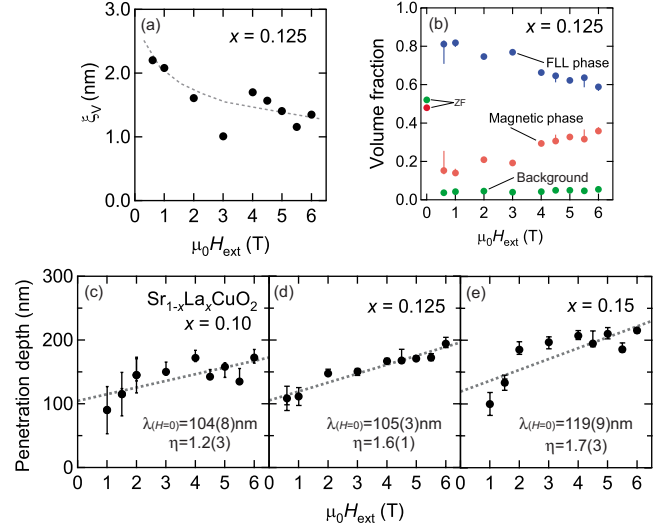


FIG. 5. (Color online) (a) Field dependence of cutoff parameter and (b) volume fraction of each phase at 2 K for the sample with $x=0.125$, where dashed curves are guide for the eyes. [(c)–(e)] Field dependence of effective penetration depth at 2 K for $x=0.10$, 0.125, and 0.15, respectively. The dashed lines are a linear fit (see text).

$$\hat{P}(t) = \hat{P}_v(t) + \hat{P}_n(t), \quad (7)$$

$$\hat{P}_v(t) \equiv f_v e^{-\sigma_p^2 t^2} \int n_v(B) e^{i(\gamma_\mu B t - \phi)} dB, \quad (8)$$

$$n_v(B) = \langle \delta[B - B_v(\mathbf{r})] \rangle_r, \quad (9)$$

where f_v is the volume fraction of FLL phase, σ_p represents the contribution from the distortion of FLL due to vortex pinning and that due to nuclear random local fields, and $\hat{P}_n(t)$ is that defined in Eq. (6). The parameters including f_v , λ , ξ_v , σ_p , f_k , σ_k , and ω_k were determined by the χ^2 -minimization method with good fits as inferred from the value of reduced χ^2 close to unity. (More specifically, in order to reduce the uncertainty for the analysis of data below T_c , ω_k was fixed to the value determined by the data above T_c .) The magnitude of line broadening due to vortex pinning (σ_p) was relatively small (typically 30%–40% of the frequency shift for the shoulder C in Fig. 4). This was partly due to relatively short λ and associated large asymmetry in $n(B)$, and thereby the correlation between these parameters turned out to be small except at lower fields ($\mu_0 H_{\text{ext}} \leq 1$ T) where the spectra exhibit stronger relaxation due to greater linewidth of $n(B)$ and stronger vortex pinning (leading to larger σ_p).

Figure 5(a) shows a decreasing tendency of ξ_v with increasing field, which is understood as a shrinkage of vortex core due to vortex-vortex interaction.¹⁹ Figure 5(b) shows the field dependence of fractional yield for each phase at 2 K. With increasing field, the FLL phase appears to be transformed into the magnetic phase. However, it must be noted that there is a discontinuous change between ZF ($\sim 50\%$) and HTF- μ SR ($\sim 60\%$ – 80%). Since no field dependence is observed for the volume fraction in the normal state (T

~ 50 K), the reduction of the magnetic fraction at lower fields is attributed to the overlap of magnetic domains with vortex cores: the magnetic domains would serve as pinning centers for vortices more effectively at lower fields due to the softness of FLL. The increase in magnetic fraction with increasing field is then readily understood as a result of decreasing probability for vortices to overlap with random magnetic domains at higher fields because the relative density of vortices as well as the rigidity of FLL would increase. This also suggests that the mean domain size of the magnetic phase is considerably smaller than the FLL spacing ($=69$ nm at 0.5 T).

Figures 5(c)–5(e) show the field dependence of λ in each compound. While the London penetration depth is a physical constant uniquely determined by local electromagnetic response, λ in our definition [Eq. (1)] is a variable parameter, as n_s depends on temperature (T) and external magnetic field (H). Therefore, we introduce an effective penetration depth, $\lambda(T, H)$, with an explicit reference to T and H dependence. It is clear in Figs. 5(c)–5(e) that $\lambda(H)=\lambda(2\text{ K}, H)$ tends to increase with increasing external field. Here, one may further notice a tendency that $\lambda(H)$ increases more steeply below ~ 2 T in the case of $x=0.10$ and 0.15. However, these points at lower fields are also associated with larger error bars probably because of the stronger depolarization in the time domain. The value extrapolated to $\mu_0 H_{\text{ext}}=0$ [$\lambda(0)$] is estimated by a linear fit with a proper consideration of the uncertainty associated with these errors, and the result is indicated in Fig. 5. These values (104–119 nm) turn out to be significantly shorter than the earlier result⁷ (hereafter, the in-plane penetration depth λ_{ab} is approximated by an equation $\lambda \approx 1.3\lambda_{ab}$, according to Ref. 26). In qualitative sense, however, our result supports the earlier suggestion of a large discrepancy for SLCO from the quasilinear relation between T_c and n_s observed over a wide variety of p -type cuprates.⁸ The anomaly becomes more evident when they are mapped to the T_c vs λ^{-2} plot, as shown in Fig. 6. They are far off the line followed by the data of p -type cuprates, suggesting that n -type SLCO belongs to a class of superconductors different from that of p -type cuprates.

It is well established that the carrier concentration, p , of p -type cuprates nearly corresponds to that of the doping value x while $x \leq 0.20$.²⁷ In contrast, a recent ARPES measurement on an n -type cuprate, $\text{Nd}_{2-x}\text{Ce}_x\text{CuO}_{4\pm\delta}$, has revealed that small electron pockets ($p \approx x$) observed for $x=0.04$ sample are replaced by a large Fermi surface (corresponding to $p \approx 1+x$) for $x=0.10$ and 0.15 samples.²⁸ When m^* is assumed to be comparable with that of p -type cuprate ($m^* \approx 3m_e$), n_s can be estimated using Eq. (1), yielding $1.3 \times 10^{22} \text{ cm}^{-3}$ in SLCO with $x=0.125$ [where $\lambda(0)$ is determined with the best accuracy]. This corresponds to $p \geq 0.70$, and an order of magnitude larger than that of p -type cuprates.^{19,29} A better correspondence to $p \approx 1+x=1.125$ would be attained when $m^* \approx 4.8m_e$. Thus, the present result is yet another evidence for a large Fermi surface in SLCO. This is also in line with some recent experimental results for n -type superconductors. For example, resistivity (ρ) in the normal state shows a Fermi-liquid-like temperature dependence ($\rho \propto T^2$) common to ordinary metals,³⁰ and a metallic Korringa law has been revealed by NMR study under high

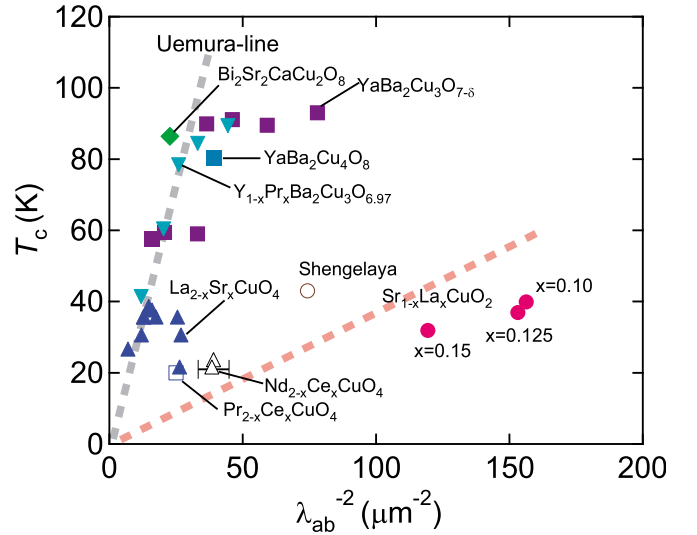


FIG. 6. (Color online) T_c vs λ^{-2} for various cuprate superconductors. The closed circles represent our result, whereas the open circle is that of Ref. 7. The open squares and triangles are for other n -type cuprates (Refs. 33–35), closed upward triangles for $\text{La}_{2-x}\text{Sr}_x\text{CuO}_4$ (Refs. 29 and 36–38) and downward ones for $\text{Y}_{1-x}\text{Pr}_x\text{Ba}_2\text{Cu}_3\text{O}_{6.97}$ (Ref. 39). The square symbols for $\text{YBa}_2\text{Cu}_3\text{O}_y$ and diamond for $\text{Bi}_2\text{Sr}_2\text{CaCu}_2\text{O}_8$ (Refs. 40–43).

magnetic fields.³¹ These observations coherently suggest that the n -type cuprates cannot be regarded as the doped Mott insulators, but they might be better understood as in the normal Fermi-liquid state already at the optimal doping ($x \sim 0.1$).

The increase in λ with increasing external field is a clear sign that the superconducting order parameter is not described by that of simple isotropic s -wave pairing for single-band electrons.¹² One of the possible origins for the field dependent λ is the presence of nodal structure in the order parameter [$|\Delta(\mathbf{k})|=0$ at particular \mathbf{k}] that leads to the field-induced quasiparticle excitation due to the quasiclassical Doppler shift.³² The quasiparticle energy spectrum is shifted by the flow of supercurrent around vortex cores to an extent $\delta E = m\mathbf{v}_F \cdot \mathbf{v}_s$, where \mathbf{v}_F and \mathbf{v}_s are the Fermi velocity and superfluid velocity, respectively. This gives rise to the pair breaking for $|\Delta(\mathbf{k})| < \delta E$ and associated reduction of n_s . The presence of nodes also leads to a nonlocal effect in which λ is affected by the modification of supercurrent near the nodes where the coherence length $\xi_0(\mathbf{k}) = \hbar v_F / \pi \Delta(\mathbf{k})$ exceeds the local London penetration depth.⁴⁴ For the comparison of magnitude for the field-induced effect, we use a dimensionless parameter η deduced by fitting data in Fig. 5 using $\lambda(h) = \lambda(0)[1 + \eta h]$ with $h = H/H_{c2}$. Provided that η is dominated by the presence of gap nodes, the magnitude of η at lower fields is roughly proportional to the phase volume of the Fermi surface where $|\Delta(\mathbf{k})| < \delta E$. As seen in Fig. 5, η in SLCO is definitely greater than zero irrespective of x , taking values between 1.2 and 1.7. It is noticeable that these values are considerably smaller than $\eta \approx 6$ ($\mu_0 H_{\text{ext}} < 2$ T) observed in $\text{YBa}_2\text{Cu}_3\text{O}_{6.95}$ (YBCO) that has a typical $d_{x^2-y^2}$ -wave gap symmetry. The situation remains true even when one considers (i) the nonlocal effect that tends to reduce η at high magnetic fields ($\eta \approx 2$ for $\mu_0 H_{\text{ext}} > 2$ T) (Ref. 45) and (ii) a

possible overestimation of λ at higher fields due to the extended use of the m -London model that also leads to the overestimation of η [e.g., η based on the m -London model is greater than that on the GL model by 0.23(7) in NbSe₂ (Ref. 19) and 0.6(2) in YB₆ (Ref. 12)].

Interestingly, the relatively small value of η is in line with the recent suggestion by ARPES measurement on another n -type superconductor, Pr_{0.89}LaCe_{0.11}CuO₄ (PLCCO), which the order parameter $\Delta(k, \psi)$ has a steeper gradient at the nodes along azimuthal (ψ) direction than that for the $d_{x^2-y^2}$ symmetry.⁶ Since the phase volume satisfying $|\Delta(\mathbf{k})| < \delta E$ is inversely proportional to $d|\Delta(k, \psi)|/d\psi$ at the node, we have

$$\eta \propto \left(\frac{d|\Delta(k, \psi)|}{d\psi} \right)_{\psi(|\Delta|=0)}^{-1}. \quad (10)$$

Assuming a situation similar to PLCCO and that η observed in YBCO represents a typical value for $d_{x^2-y^2}$ -wave gap, our result suggests that the gradient $d|\Delta(k, \psi)|/d\psi$ in SLCO is 1.2(3)–5.0(3) times greater than that at the node of $d_{x^2-y^2}$ -wave gap. However, it is clear that further assessments by other techniques that are more sensitive to the symmetry of the order parameters are necessary to discuss the details of gap structure in SLCO.

In conclusion, it has been revealed by the present μ SR study that a phase separation occurs in an electron-doped

cuprate superconductor, Sr_{1-x}La_xCuO₂ ($x=0.10, 0.125, \text{ and } 0.15$), where nearly half of the sample volume exhibits magnetism having no long-range correlation while the rest remains nonmagnetic. The superconductivity occurs predominantly in the nonmagnetic domain, where the effective magnetic penetration depth evaluated by using a modified-London model is much shorter than that of other p -type cuprates. This suggests a large carrier density corresponding to $1+x$ and accordingly the breakdown of the Mott insulating phase in SLCO and other n -type cuprates even at their optimal doping. The field dependence of λ suggests that the superconductivity of SLCO is not described by single-band s -wave pairing. The magnitude of the dimensionless parameter, η ($\propto d\lambda/dH$), is qualitatively in line with nonmonotonic d -wave superconducting gap observed in other n -type cuprates.

We would like to thank the staff of TRIUMF for technical support during the μ SR experiment and Takano-group of ICR-Kyoto University (M. Takano, Y. Shimakawa, M. Azuma, I. Yamada, and K. Oka) for useful advice concerning sample preparation. This work was partially supported by the Grant-in-Aid for Creative Scientific Research and the Grant-in-Aid for Scientific Research on Priority Areas by the Ministry of Education, Culture, Sports, Science and Technology, Japan.

*ksatoh@post.kek.jp

[†]Present address: Materials and Structures Laboratory, Tokyo Institute of Technology.

¹H. Takagi, S. Uchida, and Y. Tokura, Phys. Rev. Lett. **62**, 1197 (1989).

²F. C. Zhang and T. M. Rice, Phys. Rev. B **37**, 3759 (1988).

³For the recent review, see, for example, P. W. Anderson, P. A. Lee, M. Randeria, T. M. Rice, N. Trivedi, and F. C. Zhang, J. Phys.: Condens. Matter **16**, R755 (2004).

⁴For the recent review, see for example, T. Moriya and K. Ueda, Adv. Phys. **49**, 555 (2000).

⁵K. Yamada, K. Kurahashi, T. Uefuji, M. Fujita, S. Park, S.-H. Lee, and Y. Endoh, Phys. Rev. Lett. **90**, 137004 (2003).

⁶H. Matsui, K. Terashima, T. Sato, T. Takahashi, M. Fujita, and K. Yamada, Phys. Rev. Lett. **95**, 017003 (2005).

⁷A. Shengelaya, R. Khasanov, D. G. Eshchenko, D. Di Castro, I. M. Savić, M. S. Park, K. H. Kim, S.-I. Lee, K. A. Müller, and H. Keller, Phys. Rev. Lett. **94**, 127001 (2005).

⁸Y. J. Uemura, L. P. Le, G. M. Luke, B. J. Sternlieb, W. D. Wu, J. H. Brewer, T. M. Riseman, C. L. Seaman, M. B. Maple, M. Ishikawa, D. G. Hinks, J. D. Jorgensen, G. Saito, and H. Yamochi, Phys. Rev. Lett. **66**, 2665 (1991).

⁹K. M. Kojima, K. Kawashima, M. Fujita, K. Yamada, M. Azuma, M. Takano, A. Koda, K. Ohishi, W. Higemoto, R. Kadono, and Y. J. Uemura, Physica B (Amsterdam) **374-375**, 207 (2006).

¹⁰C.-T. Chen, P. Seneor, N.-C. Yeh, R. P. Vasquez, L. D. Bell, C. U. Jung, J. Y. Kim, M.-S. Park, H.-J. Kim, and S.-I. Lee, Phys. Rev. Lett. **88**, 227002 (2002).

¹¹Z. Y. Liu, H. H. Wen, L. Shan, H. P. Yang, X. F. Lu, H. Gao, M.-S. Park, C. U. Jung, and S.-I. Lee, Europhys. Lett. **69**, 263 (2005).

¹²R. Kadono, S. Kuroiwa, J. Akimitsu, A. Koda, K. Ohishi, W. Higemoto, and S. Otani, Phys. Rev. B **76**, 094501 (2007).

¹³R. Kadono, J. Phys.: Condens. Matter **16**, S4421 (2004).

¹⁴G. Er. S. Kikkawa, F. Kanamaru, Y. Miyamoto, S. Tanaka, M. Sera, M. Sato, Z. Hiroi, M. Takano, and Y. Bando, Physica C **196**, 271 (1992).

¹⁵K. Kawashima, M.S. thesis (unpublished).

¹⁶S. Karimoto, K. Ueda, M. Naito, and T. Imai, Physica C **378-381**, 127 (2002).

¹⁷R. Kadono, H. Okajima, A. Yamashita, K. Ishii, T. Yokoo, J. Akimitsu, N. Kobayashi, Z. Hiroi, M. Takano, and K. Nagamine, Phys. Rev. B **54**, R9628 (1996).

¹⁸E. H. Brandt, Phys. Rev. B **37**, 2349 (1988).

¹⁹J. E. Sonier, J. H. Brewer, and R. F. Kiefl, Rev. Mod. Phys. **72**, 769 (2000).

²⁰V. S. Zapf, N.-C. Yeh, A. D. Beyer, C. R. Hughes, C. H. Mielke, N. Harrison, M. S. Park, K. H. Kim, and S.-I. Lee, Phys. Rev. B **71**, 134526 (2005).

²¹S. P. Brown, D. Charalambous, E. C. Jones, E. M. Forgan, P. G. Kealey, A. Erb, and J. Kohlbrecher, Phys. Rev. Lett. **92**, 067004 (2004).

²²R. Gilardi, J. Mesot, A. Drew, U. Divakar, S. L. Lee, E. M. Forgan, O. Zaharko, K. Conder, V. K. Aswal, C. D. Dewhurst, R. Cubitt, N. Momono, and M. Oda, Phys. Rev. Lett. **88**, 217003 (2002).

²³R. Kadono, K. H. Satoh, A. Koda, T. Nagata, H. Kawano-

- Furukawa, J. Suzuki, M. Matsuda, K. Ohishi, W. Higemoto, S. Kuroiwa, H. Takagiwa, and J. Akimitsu, *Phys. Rev. B* **74**, 024513 (2006).
- ²⁴K. Ohishi, K. Kakuta, J. Akimitsu, W. Higemoto, R. Kadono, J. E. Sonier, A. N. Price, R. I. Miller, R. F. Kiefl, M. Nohara, H. Suzuki, and H. Takagi, *Phys. Rev. B* **65**, 140505(R) (2002).
- ²⁵C. M. Aegerter, S. H. Lloyd, C. Ager, S. L. Lee, S. Romer, H. Keller, and E. M. Forgan, *J. Phys.: Condens. Matter* **10**, 7445 (1998).
- ²⁶V. I. Fesenko, V. N. Gorbunov, and V. P. Smilga, *Physica C* **176**, 551 (1991).
- ²⁷Y. Fukuzumi, K. Mizuhashi, K. Takenaka, and S. Uchida, *Phys. Rev. Lett.* **76**, 684 (1996).
- ²⁸N. P. Armitage, F. Ronning, D. H. Lu, C. Kim, A. Damascelli, K. M. Shen, D. L. Feng, H. Eisaki, Z.-X. Shen, P. K. Mang, N. Kaneko, M. Greven, Y. Onose, Y. Taguchi, and Y. Tokura, *Phys. Rev. Lett.* **88**, 257001 (2002).
- ²⁹G. Aeppli, R. J. Cava, E. J. Ansaldo, J. H. Brewer, S. R. Kretzmann, G. M. Luke, D. R. Noakes, and R. F. Kiefl, *Phys. Rev. B* **35**, 7129 (1987).
- ³⁰C. H. Wang, L. Huang, L. Wang, Y. Peng, X. G. Luo, Y. M. Xiong, and X. H. Chen, *Supercond. Sci. Technol.* **17**, 469 (2004).
- ³¹G.-Q. Zheng, T. Sato, Y. Kitaoka, M. Fujita, and K. Yamada, *Phys. Rev. Lett.* **90**, 197005 (2003).
- ³²G. E. Volovik, *Pis'ma Zh. Eksp. Teor. Fiz.* **58**, 457 (1993) [*JETP Lett.* **58**, 469 (1993)].
- ³³C. C. Homes, R. P. S. M. Lobo, P. Fournier, A. Zimmers, and R. L. Greene, *Phys. Rev. B* **74**, 214515 (2006).
- ³⁴A. A. Nugroho, I. M. Sutjahja, A. Rusydi, M. O. Tjia, A. A. Menovsky, F. R. de Boer, and J. J. M. Franse, *Phys. Rev. B* **60**, 15384 (1999).
- ³⁵C. C. Homes, B. P. Clayman, J. L. Peng, and R. L. Greene, *Phys. Rev. B* **56**, 5525 (1997).
- ³⁶G. M. Luke, Y. Fudamoto, K. Kojima, M. Larkin, J. Merrin, B. Natumi, Y. J. Uemura, J. E. Sonier, T. Ito, K. Oka, M. de Andrade, M. B. Maple, and S. Uchida, *Physica C* **282-287**, 1465 (1997).
- ³⁷T. Schneider and H. Keller, *New J. Phys.* **6**, 144 (2004).
- ³⁸C. Panagopoulos, J. R. Cooper, T. Xiang, Y. S. Wang, and C. W. Chu, *Phys. Rev. B* **61**, R3808 (2000).
- ³⁹C. L. Seaman, J. J. Neumeier, M. B. Maple, L. P. Le, G. M. Luke, B. J. Sternlieb, Y. J. Uemura, J. H. Brewer, R. Kadono, R. F. Kiefl, S. R. Kretzmann, and T. M. Riseman, *Phys. Rev. B* **42**, 6801 (1990).
- ⁴⁰W. N. Hardy, D. A. Bonn, D. C. Morgan, R. Liang, and K. Zhang, *Phys. Rev. Lett.* **70**, 3999 (1993).
- ⁴¹J. E. Sonier, D. A. Bonn, J. H. Brewer, W. N. Hardy, R. F. Kiefl, and R. Liang, *Phys. Rev. B* **72**, 146501 (2005).
- ⁴²Y. J. Uemura, V. J. Emery, A. R. Moodenbaugh, M. Suenaga, D. C. Johnston, A. J. Jacobson, J. T. Lewandowski, J. H. Brewer, R. F. Kiefl, S. R. Kretzmann, G. M. Luke, T. Riseman, C. E. Stronach, W. J. Kossler, J. R. Kempton, X. H. Yu, D. Opie, and H. E. Schone, *Phys. Rev. B* **38**, 909 (1988).
- ⁴³H. Keller, W. Kündig, I. M. Savić, H. Simmler, B. Stäubli-Pümpin, M. Warden, D. Zech, P. Zimmermann, E. Kaldis, J. Karpinski, S. Rusiecki, J. H. Brewer, T. M. Riseman, and J. W. Schneider, *Physica C* **185189**, 1089 (1991).
- ⁴⁴M. H. S. Amin, I. Affleck, and M. Franz, *Phys. Rev. B* **58**, 5848 (1998).
- ⁴⁵J. E. Sonier, J. H. Brewer, R. F. Kiefl, G. D. Morris, R. I. Miller, D. A. Bonn, J. Chakhalian, R. H. Heffner, W. N. Hardy, and R. Liang, *Phys. Rev. Lett.* **83**, 4156 (1999).